Proceedings of the ASME 2023 18th International
Manufacturing Science and Engineering Conference
MSEC2023
June 12 - June 16, 2023, New Brunswick, NJ, USA

MSEC2023-104868

ONLINE COST-EFFECTIVE CLASSIFICATION OF MIXED TOOL AND MATERIAL CONDITIONS IN ULTRASONIC METAL WELDING: TOWARDS INTEGRATED MONITORING AND CONTROL

Kuan-Chieh Lu[1], Yuquan Meng[1], Zhiqiao Dong[1], Chenhui Shao[1,*]

[1]Department of Mechanical Science and Engineering, University of Illinois at Urbana-Champaign, Urbana, IL 61801, USA

ABSTRACT

Ultrasonic metal welding (UMW) is widely used in industrial applications such as electric vehicle battery manufacturing and automotive body assembly. The joint quality of UMW is sensitive to a variety of undesired yet inevitable process disturbances such as tool condition and material surface condition. Online monitoring and control capabilities are critically needed to quickly detect process anomalies and adaptively adjust process parameters, thus ensuring satisfactory joint quality and reducing process variability. While existing research has developed online quality monitoring methods for UMW, the cost-effectiveness of hardware (sensors, data acquisition equipment, and edge-computing devices) and software (computational efficiency) in a monitoring system has not been investigated systematically. The cost-effectiveness of monitoring also decides the window during which control actions can be executed, thus ultimately influencing the joint quality. This paper presents a systematic study on three factors related to cost-effectiveness: (1) sensor selection, (2) sampling rate of data acquisition, and (3) signal fraction. A method based on discrete wavelet transformation (DWT) is used for automatic feature extraction due to its effectiveness in extracting both time-domain and frequency-domain information with varying signal lengths. We develop a multi-layer perceptron (MLP) classifier to process DWT-generated features and recognize two types of welding disturbances including tool condition and material surface condition. Case studies demonstrate that combining a suitable signal fraction with a subset of sensors leads to comparable performance to using all sensors at full length. Moreover, the interaction between the sampling rate and the signal fraction is investigated. Results confirm the feasibility of building an accurate monitoring system with limited sampling rate and signal fraction, which increases the window for real-time control.

Keywords: Ultrasonic metal welding, online monitoring, real-time control, cost-effectiveness, mixed condition classification, quality control

*Corresponding author: chshao@illinois.edu

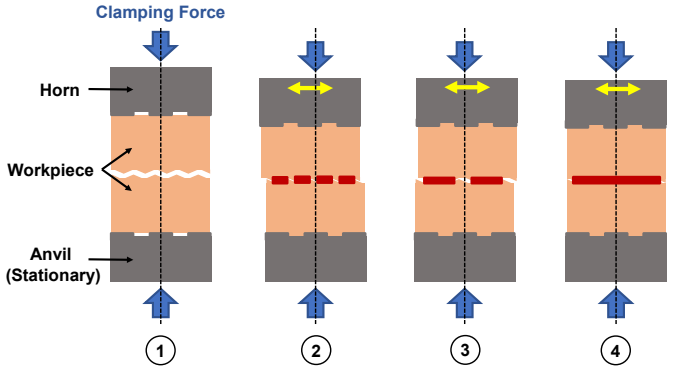

FIGURE 1: ILLUSTRATION OF AN UMW CYCLE

1. INTRODUCTION

Ultrasonic metal welding (UMW) is a solid-state welding process that is capable of joining multiple metal sheets of similar or dissimilar materials. This technique has numerous industrial applications such as automotive body construction [1, 2], lithium-ion battery manufacturing [3–5], and electronic packaging [6, 7]. A typical welding process is illustrated in Fig. 1. At the beginning of welding cycles, the clamping force generated by the pneumatic system is applied to the workpieces. Then, the horn starts vibrating at 20 kHz to remove surface oxides, expose the fresh metal, and initiate a bond. At last, the deformation layer starts growing, and the joint is formed eventually. UMW has various advantages compared to conventional fusion welding methods such as environmental friendliness, low energy consumption, and short process cycle [8–10].

One critical challenge in industrial applications of UMW lies in monitoring and controlling process variations [10–13]. UMW is sensitive to uncontrollable factors including but not limited to tool conditions [5, 14–16] and surface conditions of workpieces [17, 18]. Tool condition monitoring (TCM) for UMW is a long-standing challenge in the industry [15]. The main tools of UMW, i.e., horn and anvil, have many pyramid-shaped knurling patterns

on the surface [14, 19]. The geometrically sophisticated knurls make TCM extremely difficult since it requires a high-resolution, high-precision surface measurement system. Shao et al. [15] characterized tool wear progression and then developed an algorithm using features that are extracted from space and frequency domains of cross-sectional profiles on tool surfaces to monitor the tool condition. Zerehsaz et al. [19] proposed a high-order decomposition method to extract a low dimensional set of features from the high dimensional tool profile measurement data for detecting tool wear at an early stage. Yang et al. [20] developed a hierarchical measurement strategy to balance the interpolation precision and the measurement cost in acquiring high-resolution spatiotemporal measurements of UMW tools. To improve data efficiency and reduce measurement costs, Chen et al. [21] devised a multi-task learning approach for spatiotemporal modeling of UMW tool surface progression. Although substantial progress has been achieved in TCM, existing methods require a large amount of surface measurement data that is expensive and time-consuming to collect.

Surface condition is another common source of external disturbances in UMW. Balz et al. [22] reported the effect of the rolling direction of raw materials by using high-speed imaging to observe the relative motion between tools and samples. Nunes et al. [23] investigated the effect of surface preparation for welding copper sheets in UMW. Workpiece surface contamination is one of the most common issues on the factory floor since it reduces the friction between multiple workpieces and between workpieces and horn/anvil, which leads to unacceptable joint strength and inconsistent welding quality. Lee et al. [17] investigated the effect of surface contamination on joint strength and micro-scale weld attributes. The physical insights were then used to devise a guideline for feature selection and monitoring. Nong et al. [18] proposed a parameter adjustment method to compensate for the effect of contamination and substantially improved the robustness of UMW.

Online monitoring emerges as a promising solution to detecting variations in both tool conditions and material surface conditions. In general, online monitoring uses in-situ sensing signals and machine learning to detect process anomalies and to predict joint quality non-destructively. One stream of research in online monitoring of UMW focuses on classifying or predicting joint quality, e.g., [11, 12, 24–28]. Recently, online monitoring has been explored for detecting uncontrollable factors [29]. Nazir and Shao [16] utilized sensor fusion and machine learning to build an online TCM system for UMW. Ma et al. [30] monitored the displacement of sonotrode by a high-frequency displacement sensor and established the relationship between displacement, plastic deformation, and welding quality for multilayer UMW. Existing research on online monitoring of UMW exclusively focuses on detecting one type of conditions. The presence of mixed conditions, e.g., tool degradation and workpiece surface contamination, is more realistic yet more challenging. It is imperative to capture the interactions between different types of disturbances in such cases. Mixed condition classification remains a research gap.

The cost-effectiveness of online monitoring systems is an important factor but has not been systematically studied. The cost of a monitoring system can be categorized into hardware and time. Hardware cost is mainly induced by sensors, data acquisition devices, and computing equipment. Intuitively, using more sensors of high capability in alliance with a high sampling rate provides more data, which may potentially improve monitoring performance. However, a large data set requires more computing resources for processing/analysis and increases the time cost of monitoring. Furthermore, the time cost of monitoring also decides the control window in which the real-time controller can execute a suitable strategy to overcome process disturbances. Unfortunately, additional data does not always guarantee better monitoring performance since some data sources provide only limited insights into the physical welding process or even include misleading, irrelevant information. As such, it is imperative to develop a cost-effective monitoring system that can minimize the data, cost, and time needed to achieve high monitoring accuracy, while ensuring a sufficient control window to adjust the process online.

This paper systematically investigates the cost-effectiveness of online monitoring mixed tool and material conditions. We consider three important cost factors: (1) sensor selection, (2) sampling rate, and (3) signal fraction (i.e., the portion of a signal used for monitoring). We develop a monitoring method that consists of discrete wavelet transform (DWT)-based feature generation and multi-layer perceptron (MLP) classifier to recognize the mixed conditions of tool and surface. Then we vary the levels of data availability determined by three abovementioned factors and compare the classification accuracy. It is demonstrated that the performance of using the suitable subset of sensors at a limited signal fraction is comparable with the performance of using all sensors at full length. Moreover, the interaction between the sampling rate and the signal fraction is investigated. The outcome confirms the feasibility of building an accurate monitoring system with a limited sampling rate and signal fraction, which reduces the monitoring cost and increases the window for real-time control.

The remainder of this paper is organized as follows. Section 2 presents the online monitoring method. Section 3 presents three case studies to scrutinize the effect of factors related to cost-effectiveness. Finally, Section 4 summarizes the conclusion and suggests future research directions.

2. METHODOLOGY

2.1 Data Acquisition System

The data acquisition (DAQ) system collects sensor signals during the welding cycle. Figure 2 shows the architecture and components of the DAQ system. A National Instrument USB-6361 multi-functional DAQ device acts as a bridge between the welding machine and the computer. The computer running MATLAB script collects four signals, which are briefly introduced as follows:

1. Power signal (internal signal): Instantaneous power consumption of welder during the welding cycle.
2. Vertical displacement signal (internal signal): The vertical displacement of the horn is measured by built-in linear variable differential transformer (LVDT).
3. Acoustic emission (AE) (external signal): A Physical Acoustic - R15α AE sensor attached on the anvil assembling

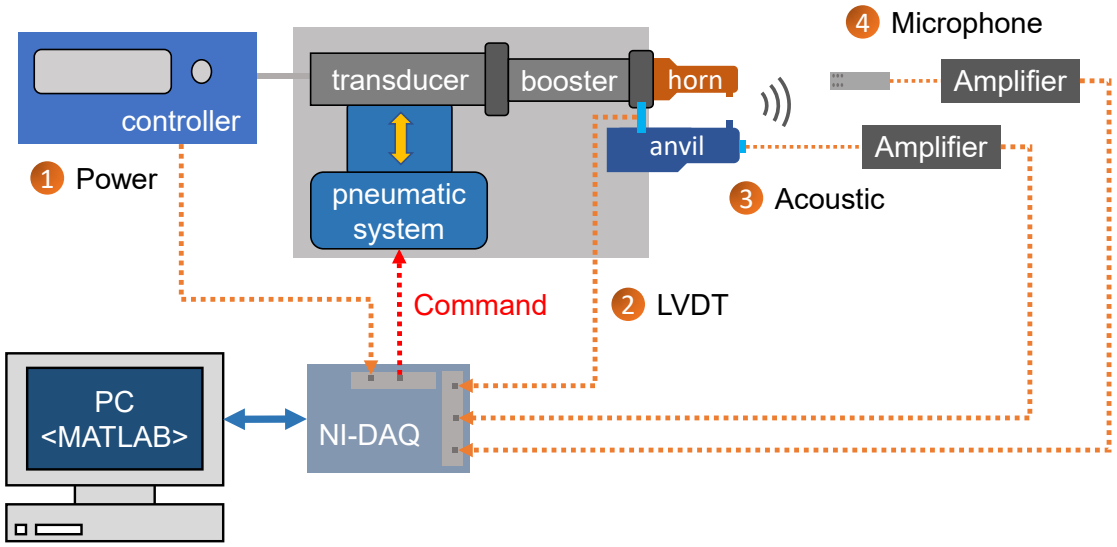

FIGURE 2: DAQ SYSTEM ARCHITECTURE

collect acoustic signal during the welding cycle. The signal is amplified by Physical Acoustic 2/4/6 voltage preamplifier.

4. Microphone (external signal): A GRAS 40PP microphone placed near the machine records sound signal during the welding cycle. The signal is amplified by GRAS 12AL preamplifier.

2.2 Monitoring Software

The monitoring software uses collected in-situ sensing signals to recognize mixed tool conditions and surface conditions. The software includes two major steps: feature generation and classification.

DWT is selected for feature generation because of its effectiveness in extracting both time-domain and frequency-domain information with varying signal lengths. Since UMW is a joining process based on high-frequency vibration, time-frequency information is important when monitoring the quality and predicting process conditions [31]. The effectiveness of DWT was first verified in a previous work [27]. As shown in Fig. 3, DWT decomposes a raw signal into detail coefficients (DCs) from high frequency and approximation coefficients (ACs) from low frequency. Then, the approximation coefficients can be decomposed again, and this process can repeat to level M_d, leading to $M_d + 1$ levels for each signal. In the case studies, we use $M_d = 12$. Then, features including statistical information, entropy, and crossings are extracted using the coefficients. The definitions of all features are summarized in Table 1. At last, all four signals go through the feature generation process and 624 (12 features $\times$ 13 levels $\times$ 4 signals) features are extracted.

An MLP classifier is built to predict the mixed condition. Since both tool conditions and surface conditions influence the welding process at the same time, it is important to capture their interactions for better accuracy. It is worth noting that the existing research is exclusively focused on single-condition prediction, and mixed condition prediction is a more challenging problem. Our preliminary study found that the proposed one-classifier method had the same or even better performance than using two separate classifiers. Nine mixed conditions from the combination of three tool conditions (new, damaged, worn) and three surface conditions (clean, polished, contaminated) are predicted by the MLP classifier. The MLP shown in Fig. 4 has three hidden layers with the rectified linear unit (ReLU) as the activation function and the adaptive moment estimation (Adam) as a solver for weight optimization. The architecture of the MLP model is selected based on our prior work [27]. It was demonstrated that the MLP model was able to achieve near-perfect performance for TCM. As such, in this research, we use the same architecture and train the model parameters using the newly collected dataset.

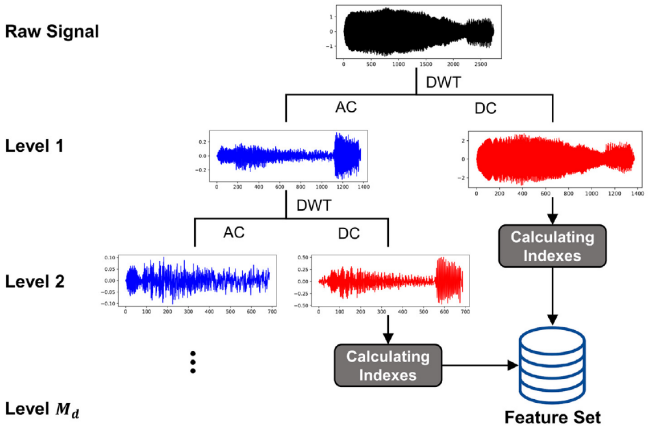

FIGURE 3: ILLUSTRATION OF USING DWT TO DECOMPOSE MICROPHONE SIGNAL FOR FEATURE EXTRACTION [27]

The average testing accuracy of 5-fold cross-validation, which is illustrated by Fig. 5, is set as the performance criterion. In each iteration of the 5-fold cross-validation procedure, a

TABLE 1: FEATURE AND DESCRIPTION

Feature	Description
Entropy	Entropy of the sub-band
Mean	Mean of the sub-band
Median	Median of the sub-band
5th percentile	5th percentile of the sub-band
25th percentile	25th percentile of the sub-band
75th percentile	75th percentile of the sub-band
95th percentile	95th percentile of the sub-band
RMS	Root-mean-square of the sub-band
Variance	Variance of the sub-band
STD	Standard deviation of the sub-band
Zero crossing rate	Rate of the sub-band crosses zero
Mean crossing rate	Rate of the sub-band crosses mean

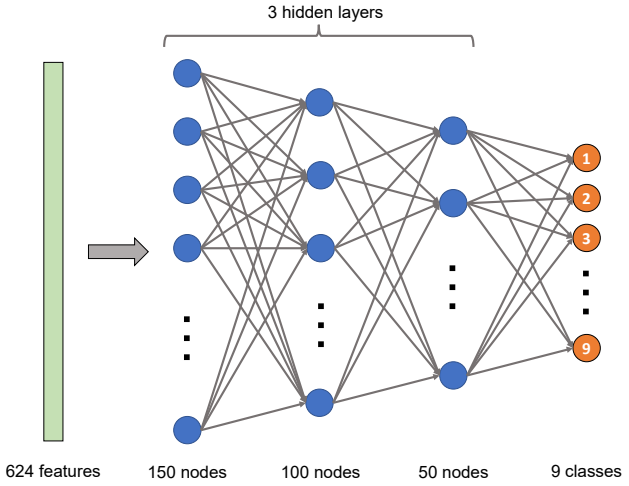

FIGURE 4: ARCHITECTURE OF THE MLP CLASSIFIER USED FOR MIXED CONDITION CLASSIFICATION

TABLE 2: TOOL AND SURFACE CONDITIONS

Label	Tool Condition	Surface Condition
1	New	Clean
2	New	Contaminated
3	New	Polished
4	Damaged	Clean
5	Damaged	Contaminated
6	Damaged	Polished
7	Worn	Clean
8	Worn	Contaminated
9	Worn	Polished

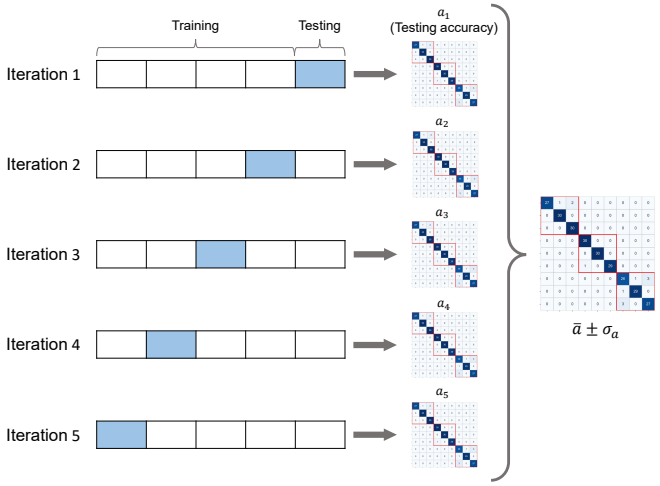

FIGURE 5: PROCESS OF 5-FOLD CROSS VALIDATION

new model is trained with the corresponding training set. There is no information exchange between iterations, which means that all models are trained independently without the worry of data leakage. By letting all samples occur once in the testing set, we eliminate the selection bias that may result from doing a single train-test split, thus improving the robustness of our results.

2.3 Experimental Setup

In industrial applications of UMW, tool conditions are typically evaluated by disassembling the tools from the welder and measuring the surface using high-resolution metrology [15, 19]. It is also necessary to re-assemble the tools to resume production. This practice disrupts the production and leads to substantial production downtime and significant delay in maintenance decision-making. Therefore, online TCM is preferred to achieve responsive and cost-effective decision-making. Surface conditions are an uncontrollable factor since contamination like cutting fluid is hard to remove completely, especially on the factory floor. As a result, tool and surface conditions are not known in advance, and it is important to detect and classify these disturbances for the purposes of monitoring and control.

UMW experiments were conducted under the combination of three surface conditions and three tool conditions as shown in Table 2. A "new" tool refers to a set of a horn and an anvil with fresh knurl patterns. After thousands of welding cycle, the tool wears out in the forms of knurl pattern changes [14, 15]. A "damaged" tool is a result of an undesired collision between the horn and anvil, which cause abnormal wear to the knurl pattern. For the surface condition, the workpiece cleaned with alcoholic wipes is defined as a "clean" surface. A "polished" surface means that the contact faces of the workpiece are polished with sandpaper before welding. At last, a "contaminated" condition is created by applying one drop of cutting fluid to the welding area.

With nine mixed conditions and 30 replicates for each condition combination, 270 samples are collected. The workpiece specification and welding parameters shown in Table 3 are fixed during the welding. The raw signals of four sensors (power, LVDT, AE, and microphone) is collected at 200 kHz. Figure 6 shows an example of collected raw signals and the definition of the signal fraction. The signal fraction is defined as the ratio of the signal segment used for monitoring to the full-length signal. Given the physical constraints of the integrated monitoring and control system, the signal segment has to be continuously counted from the beginning of a welding cycle and all four signals should

TABLE 3: PROCESS PARAMETERS AND WORKPIECE DIMENSION

Parameter	Setting
Vibration amplitude	40 µm
Clamping pressure	50 psi
Welding time	1 second
Sample size	50.8 mm x 25.4 mm
Sample material	0.2 mm thick copper

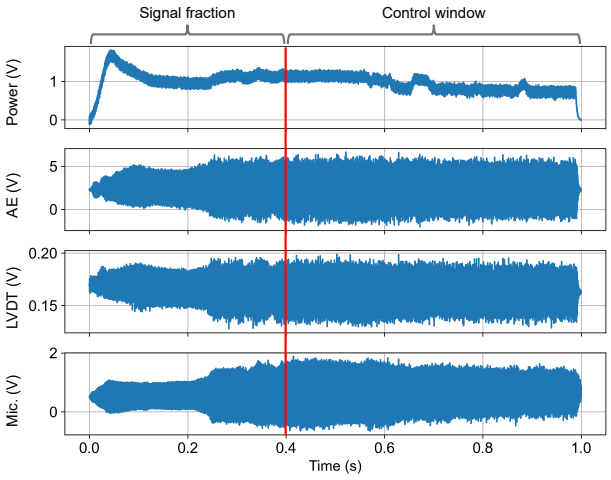

FIGURE 6: EXAMPLE OF RAW SIGNAL, SIGNAL FRACTION, AND CONTROL WINDOW

use the same signal fraction. A smaller signal fraction implies that we identify the mixed condition earlier and reserve more time for the control window. For example, a signal fraction of 40% means that the first continuous 40% of all four signals are used for monitoring and the control algorithm is given 60% of the total welding time for process adjustment.

3. CASE STUDY

Three systematic case studies are designed to investigate: (1) sensor selection (2) sampling rate of data acquisition, and (3) signal fraction. The purpose of the first case study is to select the appropriate sensors for the monitoring system. Superior data efficiency translates into using fewer sensors while achieving high classification accuracy. Then, the second case study scrutinizes the effect of signal fraction, and classification errors are studied in detail discussion. At last, the interaction between the sampling rate and the signal fraction is investigated in the third case study.

3.1 Sensor Selection

The performance of using all four sensors is set as a benchmark, and the performance of using only selected sensors is compared to the benchmark. First, the performance of using only one sensor is evaluated at various signal fractions. As we can see in Fig. 7, the power signal has the best performance while the AE signal comes in the second place. When the signal fraction is less than 50%, the benchmark does outperform the power signal. However, the power signal can achieve 90% accuracy when using

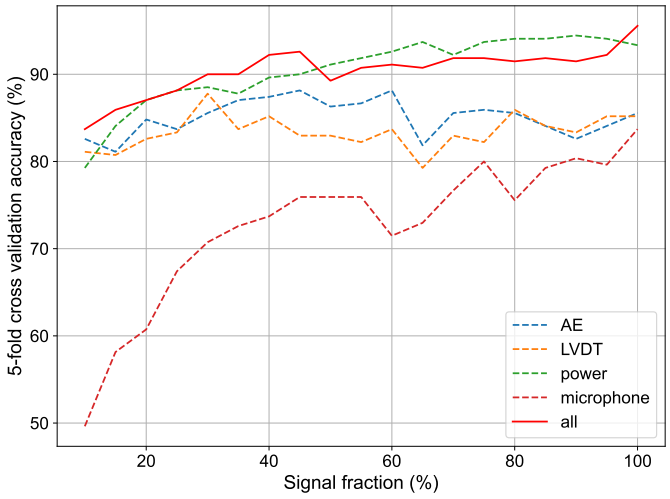

FIGURE 7: SINGLE SENSOR SELECTION

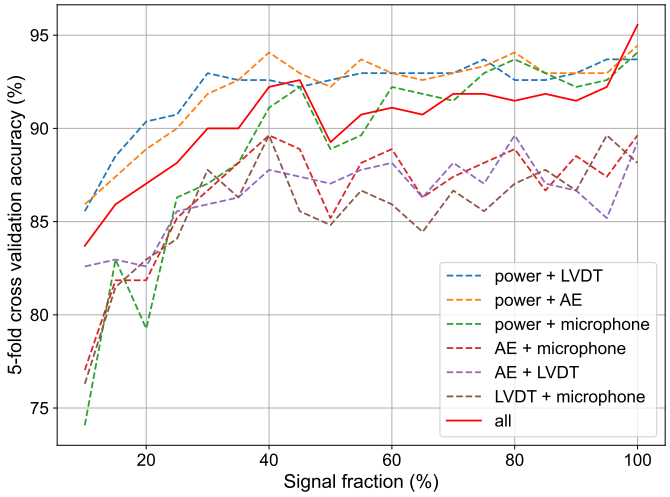

FIGURE 8: SENSOR FUSION PAIRS SELECTION

only 40% of the signal length. Moreover, the power signal has better performance than the benchmark when the signal fraction is larger than 50%, which indicates that an internal sensor is sufficient and the cost of using external sensors can be avoided. This phenomenon is strong evidence that choosing a sensor wisely can lead to higher data efficiency while using more sensors might provide misleading information for the classifier.

Then, we are interested in the performance of sensor fusion. Sensor signals are tested pair by pair, and the result is compared to the benchmark as well. Figure 8 shows that two pairs of sensors, namely, power+LVDT and power+acoustic, have better performance than the benchmark. These two pairs of sensors have great performance even when the signal fraction is extremely low, and they reach 90% accuracy when using only a signal fraction of 30%. The result from sensor fusion matches the result from using a single sensor. The power signal is the best when using one sensor and is the common signal in two pairs of sensor fusion. Table 4 compares the average testing accuracy and the standard deviation between power+LVDT and the benchmark. We can

TABLE 4: 5-FOLD CROSS-VALIDATION ACCURACY FOR VARIED SIGNAL FRACTIONS WHEN POWER AND LVDT SIGNALS ARE USED

Signal fraction	power + LVDT	Benchmark
0.2	0.90 ± 0.025	0.87 ± 0.075
0.4	0.93 ± 0.0	0.92 ± 0.038
0.6	0.93 ± 0.014	0.91 ± 0.018
0.8	0.93 ± 0.017	0.92 ± 0.045
1	0.94 ± 0.038	0.96 ± 0.025

see that the average testing accuracy of power+LVDT pair is higher when using limited data. Moreover, the smaller standard deviation indicates that the performance of power+LVDT is more consistent between validation folds.

From this case study, we have two important findings. First, selecting suitable sensors can identify the accurate mixed condition with only limited data. This means that cost-effective early event detection is feasible, and the small signal fraction ensures the control window is wide enough to adjust the parameter accordingly. The second interesting finding is the fact that the power+LVDT pair, both internal signals, can outperform the benchmark and other pairs of signals including an external sensor. This suggests that using built-in sensors for monitoring is sufficient thus the cost of extra sensors can be reduced significantly.

3.2 Effect of Signal Fraction

This case study focuses on analyzing the classification error under different signal fractions. The raw signal of four sensors is used for classification. In Fig. 5, the final confusion matrix is a simple superposition of 5 matrices from 5 iterations in the cross-validation. Three confusion matrices from select signal fractions are shown in Fig. 9.

In Fig. 9a, we can see that using a full-length signal can achieve 96% accuracy. Three sub-matrices present the classification results of three tool conditions. It is shown that the classifier can identify the tool condition perfectly while most of the errors come from the confusion between different surface conditions. Besides, there is a trend showing that the confusion between surface conditions is most obvious when using a worn tool. This phenomenon may be attributed to the fact that a worn tool leads to an abnormal process and makes the joint quality more inconsistent. It is worth noting that these patterns are consistent with the case where a lower signal fraction is used. Fig. 9b shows that the overall accuracy is 92% when the signal fraction is 40%, suggesting that excellent classification accuracy can be achieved with limited data. Fig. 9c shows that when using only 10% of the data the classification accuracy is reduced compared to larger signal fractions. However, even in this case, the classifier still correctly identifies most tool conditions.

Figure 10 presents the changes in computation time for DWT feature extraction and testing accuracy when signal fraction is varied. A roughly linear trend is observed for computation time. The computation time for DWT feature extraction when using 40% of the signal and the full signal is 54 ms and 85 ms, respectively. Using 40% of the signal saves 36.5% of the computing time.

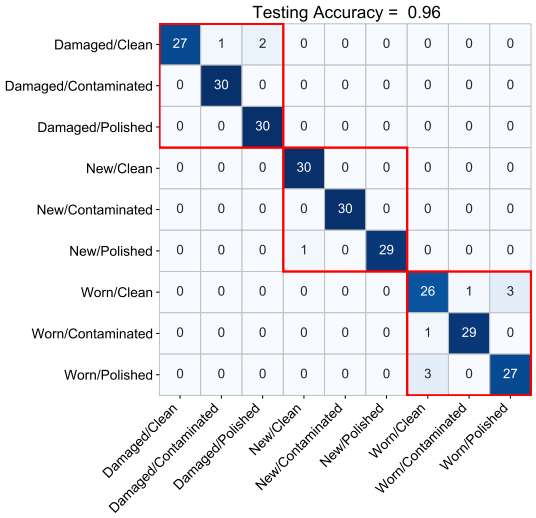

(a) Signal fraction = 100%

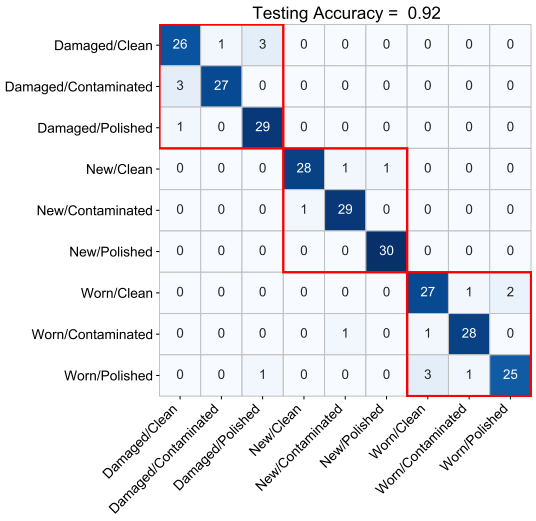

(b) Signal fraction = 40%

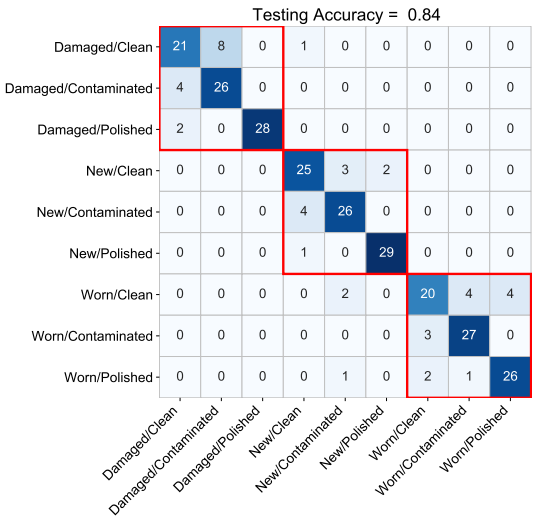

(c) Signal fraction = 10%

FIGURE 9: CONFUSION MATRIX OF 5-FOLD CROSS VALIDATION

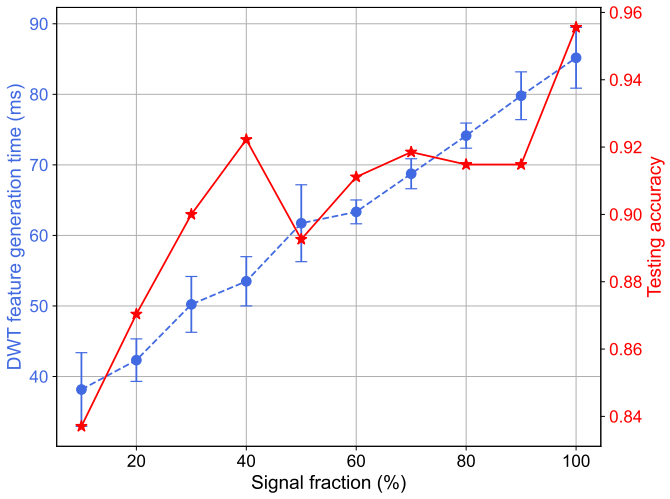

FIGURE 10: COMPUTATION TIME FOR DWT FEATURE GENERATION AND TESTING ACCURACY WITH VARIED SIGNAL FRACTION

When the signal fraction increases, the testing accuracy first improves quickly, then stabilizes, and finally increases again when the full signal length is used. This indicates that one can achieve a trade-off between computation time, which is inversely related to the control window, and monitoring accuracy. In the case of Fig. 10, a 40% signal fraction is a good choice.

3.3 Sampling Rate and Signal Fraction

The last case study investigates the interaction between signal fraction and sampling rate. The raw signal is sampled at 200 kHz and we down-sample it by several levels and test the down-sampled signal under various signal fractions. Within each combination of down sampling rate and signal fraction, DWT decomposes the signal at the maximum possible level to extract all detailed information.

Figure 11 displays the average testing accuracy with different combinations of signal fraction and sampling rate. As we can see, there is a global trend in the diagonal direction from bottom-left to top-right. When using an extremely low signal fraction at a low sampling rate, the classifier has trouble identifying the mixed condition. If we increase the signal fraction or sampling rate, which feeds more information into the classifier, the performance starts improving. The pattern demonstrates the necessity of more data if better performance is desired, which implies higher hardware and time cost. However, the performance does not increase proportionally to the data availability. If we choose the suitable combination of signal fraction and sampling rate, we can have equal or even better performance than the benchmark (200 kHz raw signal with 100% signal fraction). Moreover, the signal fraction and sampling rate can supplement each other. For example, if the signal fraction is limited to enable wider control window, a higher sampling rate can be used to achieve a high classification accuracy.

In the real-world scenario, we can achieve cost-effective monitoring and in-process control by utilizing the data wisely. In the first step, we select a range of sampling rates for reasonable hardware cost and a range of signal fractions for a feasible con-

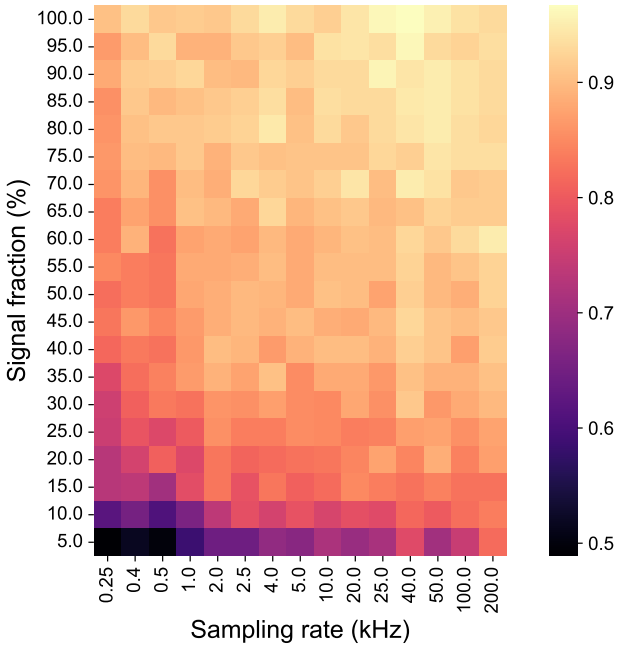

FIGURE 11: AVERAGE TESTING ACCURACY WITH VARYING SAMPLING RATES AND SIGNAL FRACTIONS

trol window. Then, we can optimize the combination of signal fraction and sampling rate for classifying the mixed condition accurately. Finally, the real-time controller can adaptively adjust the parameter to compensate for the disturbance caused by tool conditions and surface conditions.

4. CONCLUSION AND FUTURE WORK

This paper investigates the cost-effectiveness of the online UMW monitoring system with a focus on classifying mixed tool and material surface conditions. The developed MLP classifier is shown to be effective in classifying nine mixed conditions with high accuracy, thus offering a new capability for detecting process disturbances in complicated production scenarios. The presented case studies show that only using internal signals including power and LVDT signals is sufficient to predict the mixed conditions of tools and surfaces even when data is limited. Therefore, the cost associated with hardware can be greatly reduced while maintaining good monitoring performance. The fact that the classifier can achieve high classification accuracy with low signal fraction demonstrates the feasibility of reserving a wider control window for real-time control. Furthermore, choosing a suitable combination of sampling rate and signal fraction can increase the monitoring cost-effectiveness. The capability of MLP classifier with DWT-generated features is proven and it can serve as an essential element for in-process monitoring and early event detection.

In the future, the developed cost-efficient monitoring method can be used to facilitate an effective integration of online monitoring and real-time control. We will apply the developed method to the online monitoring system for early, cost-effective recognition of the mixed conditions. Then, a control strategy will be devised to generate the control input (e.g., change in clamping pressure) accordingly. Finally, the real-time controller will adaptively ad-

just the pneumatic system to compensate for the disturbances, thus promoting joint quality.

ACKNOWLEDGMENTS

This research has been supported by the National Science Foundation under Grant No. 1944345.

REFERENCES

[1] Siddiq, A. and Ghassemieh, E. "Thermomechanical analyses of ultrasonic welding process using thermal and acoustic softening effects." *Mechanics of Materials* Vol. 40 (2008): pp. 982–1000. DOI 10.1016/J.MECHMAT.2008.06.004.

[2] Ni, Z. L. and Ye, F. X. "Ultrasonic spot welding of aluminum alloys: A review." *Journal of Manufacturing Processes* Vol. 35 (2018): pp. 580–594. DOI 10.1016/J.JMAPRO.2018.09.009.

[3] Cai, Wayne W. *Ultrasonic welding of lithium-ion batteries*. ASME press (2017).

[4] Kim, T. H., Yum, J., Hu, S. J., Spicer, J. P. and Abell, J. A. "Process robustness of single lap ultrasonic welding of thin, dissimilar materials." *CIRP Annals* Vol. 60 (2011): pp. 17–20. DOI 10.1016/J.CIRP.2011.03.016.

[5] Balz, Isabel, Abi Raad, E, Rosenthal, E, Lohoff, R, Schiebahn, A, Reisgen, U and Vorländer, M. "Process monitoring of ultrasonic metal welding of battery tabs using external sensor data." *Journal of Advanced Joining Processes* Vol. 1 (2020): p. 100005.

[6] Daniels, H. P.C. "Ultrasonic welding." *Ultrasonics* Vol. 3 (1965): pp. 190–196. DOI 10.1016/0041-624X(65)90169-1.

[7] Kim, Jongbaeg, Chiao, Mu and Lin, Liwei. "Ultrasonic bonding of In/Au and Al/Al for hermetic sealing of MEMS packaging." *Proceedings of the IEEE Micro Electro Mechanical Systems (MEMS)* (2002): pp. 415–418DOI 10.1109/MEMSYS.2002.984291.

[8] Martinsen, Kristian, Hu, SJ and Carlson, BE. "Joining of dissimilar materials." *Cirp Annals* Vol. 64 No. 2 (2015): pp. 679–699.

[9] Kumar, S, Wu, CS, Padhy, GK and Ding, W. "Application of ultrasonic vibrations in welding and metal processing: A status review." *Journal of manufacturing processes* Vol. 26 (2017): pp. 295–322.

[10] Cheng, XM, Yang, K, Wang, J, Xiao, WT and Huang, SS. "Ultrasonic system and ultrasonic metal welding performance: A status review." *Journal of Manufacturing Processes* Vol. 84 (2022): pp. 1196–1216.

[11] Shao, Chenhui, Paynabar, Kamran, Kim, Tae Hyung, Jin, Jionghua Judy, Hu, S Jack, Spicer, J Patrick, Wang, Hui and Abell, Jeffrey A. "Feature selection for manufacturing process monitoring using cross-validation." *Journal of Manufacturing Systems* Vol. 32 No. 4 (2013): pp. 550–555.

[12] Guo, Weihong, Shao, Chenhui, Kim, Tae Hyung, Hu, S. Jack, Jin, Jionghua, Spicer, J. Patrick and Wang, Hui. "Online process monitoring with near-zero misdetection for ultrasonic welding of lithium-ion batteries: An integration of univariate and multivariate methods." *Journal of Manufacturing Systems* Vol. 38 (2016): pp. 141–150. DOI 10.1016/J.JMSY.2016.01.001.

[13] Xi, Liang, Banu, Mihaela, Jack Hu, S, Cai, Wayne and Abell, Jeffrey. "Performance prediction for ultrasonically welded dissimilar materials joints." *Journal of Manufacturing Science and Engineering* Vol. 139 No. 1 (2017).

[14] Shao, Chenhui, Guo, Weihong, Kim, Tae H, Jin, Jionghua Judy, Hu, S Jack, Spicer, J Patrick and Abell, Jeffrey A. "Characterization and monitoring of tool wear in ultrasonic metal welding." *9th international workshop on microfactories*: pp. 161–169. 2014.

[15] Shao, Chenhui, Kim, Tae Hyung, Hu, S. Jack, Jin, Jionghua, Abell, Jeffrey A. and Spicer, J. Patrick. "Tool Wear Monitoring for Ultrasonic Metal Welding of Lithium-Ion Batteries." *Journal of Manufacturing Science and Engineering, Transactions of the ASME* Vol. 138 (2016). DOI 10.1115/1.4031677.

[16] Nazir, Qasim and Shao, Chenhui. "Online tool condition monitoring for ultrasonic metal welding via sensor fusion and machine learning." *Journal of Manufacturing Processes* Vol. 62 (2021): pp. 806–816. DOI 10.1016/J.JMAPRO.2020.12.050.

[17] Lee, S. Shawn, Shao, Chenhui, Kim, Tae Hyung, Hu, S. Jack, Kannatey-Asibu, Elijah, Cai, Wayne W., Spicer, J. Patrick and Abell, Jeffrey A. "Characterization of ultrasonic metal welding by correlating online sensor signals with weld attributes." *Journal of Manufacturing Science and Engineering* Vol. 136 (2014). DOI 10.1115/1.4028059.

[18] Nong, Lihang, Shao, Chenhui, Kim, Tae Hyung and Hu, S. Jack. "Improving process robustness in ultrasonic metal welding of lithium-ion batteries." *Journal of Manufacturing Systems* Vol. 48 (2018): pp. 45–54. DOI 10.1016/J.JMSY.2018.04.014.

[19] Zerehsaz, Yaser, Shao, Chenhui and Jin, Jionghua. "Tool wear monitoring in ultrasonic welding using high-order decomposition." *Journal of Intelligent Manufacturing* Vol. 30 No. 2 (2019): pp. 657–669.

[20] Yang, Yuhang, Zhang, Yifang, Cai, Y. Dora, Lu, Qiyue, Koric, Seid and Shao, Chenhui. "Hierarchical measurement strategy for cost-effective interpolation of spatiotemporal data in manufacturing." *Journal of Manufacturing Systems* Vol. 53 (2019): pp. 159–168. DOI 10.1016/J.JMSY.2019.09.009.

[21] Chen, Haotian, Yang, Yuhang and Shao, Chenhui. "Multitask learning for data-efficient spatiotemporal modeling of tool surface progression in ultrasonic metal welding." *Journal of Manufacturing Systems* Vol. 58 (2021): pp. 306–315.

[22] Balz, I., Raad, E. Abi, Rosenthal, E., Lohoff, R., Schiebahn, A., Reisgen, U. and Vorländer, M. "Process monitoring of ultrasonic metal welding of battery tabs using external sensor data." *Journal of Advanced Joining Processes* Vol. 1 (2020): p. 100005. DOI 10.1016/j.jajp.2020.100005. URL https://doi.org/10.1016/j.jajp.2020.100005.

[23] Nunes, Rafael, Faes, Koen, De Meester, Sylvia, De Waele, Wim and Kubit, Andrzej. "Influence of welding parameters and surface preparation on thin copper–copper sheets

welded by ultrasonic welding process." *The International Journal of Advanced Manufacturing Technology* (2022): pp. 1–16.

[24] Lee, S. Shawn, Kim, Tae Hyung, Hu, S. Jack, Cai, Wayne W. and Abell, Jeffrey A. "Analysis of Weld Formation in Multilayer Ultrasonic Metal Welding Using High-Speed Images." *Journal of Manufacturing Science and Engineering, Transactions of the ASME* Vol. 137 (2015). DOI 10.1115/1.4029787/376337.

[25] Mongan, Patrick G, Hinchy, Eoin P, O'Dowd, Noel P and McCarthy, Conor T. "Quality prediction of ultrasonically welded joints using a hybrid machine learning model." *Journal of Manufacturing Processes* Vol. 71 (2021): pp. 571–579.

[26] Shi, Xinhua, Li, Lin, Yu, Suiran and Yun, Lingxiang. "Process Monitoring in Ultrasonic Metal Welding of Lithium Batteries by Power Signals." *Journal of Manufacturing Science and Engineering* (2021): pp. 1–22DOI 10.1115/1.4052704.

[27] Meng, Yuquan and Shao, Chenhui. "Physics-informed ensemble learning for online joint strength prediction in ultrasonic metal welding." *Mechanical Systems and Signal Processing* Vol. 181 (2022). DOI 10.1016/j.ymssp.2022.109473.

[28] Schwarz, Elisabeth Birgit, Bleier, Fabian, Guenter, Friedhelm, Mikut, Ralf and Bergmann, Jean Pierre. "Improving process monitoring of ultrasonic metal welding using classical machine learning methods and process-informed time series evaluation." *Journal of Manufacturing Processes* Vol. 77 (2022): pp. 54–62.

[29] Wang, Baicun, Hu, S Jack, Sun, Lei and Freiheit, Theodor. "Intelligent welding system technologies: State-of-the-art review and perspectives." *Journal of Manufacturing Systems* Vol. 56 (2020): pp. 373–391.

[30] Ma, Zunnong and Zhang, Yansong. "Characterization of multilayer ultrasonic welding based on the online monitoring of sonotrode displacement." *Journal of Manufacturing Processes* Vol. 54 (2020): pp. 138–147. DOI 10.1016/j.jmapro.2020.03.007.

[31] Wu, Yulun, Meng, Yuquan and Shao, Chenhui. "End-to-end online quality prediction for ultrasonic metal welding using sensor fusion and deep learning." *Journal of Manufacturing Processes* Vol. 83 (2022): pp. 685–694. DOI 10.1016/J.JMAPRO.2022.09.011.

[32] Lee, Dongkyun, Kannatey-Asibu Jr, Elijah and Cai, Wayne. "Ultrasonic welding simulations of multiple, thin and dissimilar metals for battery joining." *International Symposium on Flexible Automation*, Vol. 45110: pp. 573–584. 2012. American Society of Mechanical Engineers.

[33] Meng, Yuquan, Rajagopal, Manjunath, Kuntumalla, Gowtham, Toro, Ricardo, Zhao, Hanyang, Chang, Ho Chan, Sundar, Sreenath, Salapaka, Srinivasa, Miljkovic, Nenad, Ferreira, Placid, Sinha, Sanjiv and Shao, Chenhui. "Multi-objective optimization of peel and shear strengths in ultrasonic metal welding using machine learning-based response surface methodology." *Mathematical Biosciences and Engineering* Vol. 17 No. 6 (2020).

[34] Zhao, Dewang, Ren, Daxin, Zhao, Kunmin, Pan, Sun and Guo, Xinglin. "Effect of welding parameters on tensile strength of ultrasonic spot welded joints of aluminum to steel–By experimentation and artificial neural network." *Journal of Manufacturing processes* Vol. 30 (2017): pp. 63–74.

[35] Müller, FW, Schiebahn, A and Reisgen, U. "Quality prediction of disturbed ultrasonic metal welds." *Journal of Advanced Joining Processes* Vol. 5 (2022): p. 100086.